FASEB BioAdvances

RESEARCH ARTICLE OPEN ACCESS

Protective Effects of Rat Bone Marrow Mesenchymal Stem Cells-Derived Fusogenic Plasma Membrane Vesicles Containing VSVG Protein Mediated Mitochondrial Transfer on Myocardial Injury In Vitro

Xin Liu[1] | Hong Bian[2] | Tingyuan Zhou[1] | Chunjuan Zhao[3]

[1]Biochemistry and Molecular Biology, Basic Medical Institute of Ningxia Medical University, Yinchun, Ningxia, China | [2]Cardiothoracic Surgery, Southern University of Science and Technology Hospital, Shenzhen and Guangzhou, Guangdong, China | [3]Rehabilitation Medicine, General Hospital of Ningxia Medical University, Yinchun, Ningxia, China

Correspondence: Xin Liu (xin202407@163.com) | Hong Bian (bianhong2024@163.com)

Received: 25 November 2024 | **Revised:** 19 March 2025 | **Accepted:** 28 March 2025

Funding: This work was supported by the Natural Science Foundation of Ningxia Hui Autonomous Region (No. 2022AAC03129), the Key Scientific Research Projects of Natural Science of Ningxia Medical University in 2021 (No. XT2021003), and Shenzhen Nanshan District Health Science and Technology Project (No. NS2023056).

Keywords: fusogenic plasma membrane vesicles | mitochondria | myocardial injury | rat bone marrow mesenchymal stem cells | VSVG

ABSTRACT

Overexpression of spike glycoprotein G of vesicular stomatitis virus (VSVG) can induce the release of fusogenic plasma membrane vesicles (fPMVs), which can transport cytoplasmic, nuclear, and surface proteins directly to target cells. This study aimed to investigate the roles of rat bone marrow mesenchymal stem cells (rBMSCs)-derived fPMVs containing VSVG protein in myocardial injury and their related mechanisms. The plasmids of pLP-VSVG were used to transfect rBMSCs, and then fPMVs were obtained by mechanical extrusion. After that, H9c2 cells were first treated with hypoxia reoxygenation (HR) to establish a cardiomyocyte injury model, and then were treated with fPMVs to evaluate the rescue of rBMSCs-derived fPMVs on HR-induced cardiomyocyte injury. FPMVs containing VSVG protein were successfully prepared from rBMSCs with VSVG overexpression. Compared with control fPMVs, *ACTB*, *HDAC1*, VSVG, CD81, MTCO1, and TOMM20 were significantly up-regulated ($p < 0.05$), while eEF2 was significantly down-regulated ($p < 0.05$) in the fPMVs containing VSVG protein. Additionally, it was obvious fPMVs could carry mitochondria into H9c2 cells, and HR treatment significantly inhibited viability and induced apoptosis of H9c2 cells, as well as significantly increased the contents of TNF-α and IL-1β, and ROS levels both in cells and cellular mitochondria, while evidently reducing the levels of ATP, MRCC IV, and *MT-ND1* ($p < 0.05$). However, fPVMs could remarkably reverse the changes in these indexes caused by HR ($p < 0.05$). RBMSCs-derived fPMVs containing VSVG protein may have protective effects on myocardial injury by mediating mitochondrial transfer and regulating mitochondrial functions.

Xin Liu and Hong Bian: Co-first authors.

1 | Introduction

Despite improvements in cardiovascular care in recent decades, cardiovascular disease (CVD) remains the leading cause of death worldwide [1]. According to the data reported by the American Heart Association, more than 26 million adults in the United States have CVD, excluding high blood pressure, and an average of one CVD-related death occurs every 38 s [2, 3]. Among these deaths, deaths due to ischemic heart disease increased by about 41.7% from 1990 to 2013 [4]. Myocardial ischemia occurs when blood flow to the heart muscle is insufficient, resulting in insufficient oxygen, glucose, and other nutrients that can support oxidative phosphorylation of mitochondria [5]. After an ischemic attack, reperfusion therapy is considered to be the most effective measure to rescue ischemic heart disease [6]. However, myocardial ischemia–reperfusion therapy may induce oxidative stress and lead to ultrastructural damage and myocardial cell dysfunction, thus aggravating ischemic myocardial injury [7]. Many researchers have discussed the issue of optimizing the treatment of myocardial injury, but the underlying mechanisms and drug targets of myocardial injury remain to be elucidated [8]. Therefore, there is an urgent need to develop new drugs or other effective targets to intervene and treat myocardial injury.

Mesenchymal stem cells (MSCs) are pluripotent stem cells located in adult tissues (such as bone marrow), as well as have the ability to self-renew and differentiate into different cells, such as chondrocytes, adipocytes, osteoblasts, and myocytes [9]. Pang et al. demonstrated that bone marrow mesenchymal stem cells (BMSCs) application could effectively alleviate myocardial ischemia–reperfusion injury in mice by inducing Treg activation, particularly in the spleen [10]. Another study illustrated that BMSCs-derived exosomes carrying miR-125b could prevent myocardial ischemia–reperfusion injury through targeting SIRT7 [11]. These indicate that BMSCs have a protective effect on myocardial injury. Accumulating evidence has revealed that the therapeutic benefits of MSCs in various diseases can be attributed to their immunomodulatory properties, regenerative capacity, low immunogenicity, as well as paracrine effects [12]. Although MSCs have great potential to treat a variety of diseases, recent studies have shown that MSCs also contribute to tumor pathogenesis by supporting the tumor microenvironment, increasing tumor growth, and inhibiting anti-tumor immune responses [13, 14]. A small percentage of transplanted MSCs may die shortly after injection, and secrete extracellular vesicles and apoptotic bodies [15]. In addition, MSCs may transdifferentiate into undesirable cell types [16], which may compromise the physiological functions of the target tissues. Therefore, searching for alternatives to MSCs for the therapy of myocardial injury is crucial.

Extracellular vesicles (EVs), including exosomes and microvesicles (MV), can be used as a means of intercellular communication to transfer biologically active macromolecules, which have been widely studied [17, 18]. However, a previous study obtained a novel substance, plasma membrane vesicles (PMVs) by mechanical extrusion and found that BMSCs-derived PMVs were able to deliver cytoplasmic contents to the gastrocnemius muscle of mice [19]. In addition, overexpression of spike glycoprotein G of vesicular stomatitis virus (VSVG) has been shown to induce the release of fusogenic vesicles, which are capable of transporting cytoplasmic, nuclear, and surface proteins directly to target cells [20, 21]. A study by Lin et al. prepared fusogenic PMVs (fPMVs) containing VSVG protein, as well as found that fPMVs could be endocytosed by target cells and efficiently deliver cytoplasmic proteins and mitochondria [22]. Another research manifested that PMVs from human umbilical cord MSCs could be used as a novel stem cell therapy for the treatment of acetaminophen-induced liver injury [16]. These reports imply PMVs may effectively transfer bioactive macromolecules and mitochondria, as well as have a protective effect against tissue damage. However, the roles of fPMVs containing VSVG protein in myocardial injury are still unclear.

Previous studies have used the method of hypoxia reoxygenation (HR) to induce cardiomyocyte injury in vitro [23, 24]. Therefore, in this study, rat BMSCs (rBMSCs) with VSVG overexpression were constructed, and fPMVs containing VSVG protein were isolated. After that, cardiomyocytes H9c2 were employed to establish a cardiomyocyte injury model, and then were treated with fPMVs to investigate the effects of fPMVs on myocardial injury and their related mechanisms. This study will help to improve our understanding of fPMVs and provide a new strategy for the treatment of myocardial injury.

2 | Materials and Methods

2.1 | Cell Culture and Cell Transfection

Rat bone marrow mesenchymal stem cells (rBMSCs) and cardiomyocytes H9c2 were purchased from Cyagen Biosciences Inc. (Guangzhou, China) and Cell Bank of Academy of Chinese Sciences (Shanghai, China), respectively. Among them, rBMSCs were maintained in α-MEM medium (Servicebio, Wuhan, China) supplemented with 10% fetal bovine serum (FBS, Thermo Fisher Scientific, Waltham, MA, USA) and 1% penicillin/streptomycin (Thermo Fisher Scientific), while H9c2 cells were maintained in dulbecco's modified eagle medium (DMEM, Thermo Fisher Scientific) with 10% FBS. The rBMSCs and H9c2 cells were both cultured in an incubator with 5% CO_2 at 37°C.

The plasmids of pLP-VSVG, pDSRed-Express2-N1, and pMito-GFP were prepared and provided by Yanzai Biotechnology (Shanghai, China). The cell transfection was performed using Lipofectamine 2000 (Thermo Fisher Scientific) based on the manufacturer's protocols. Briefly, the cell medium was changed to serum-free medium, and rBMSCs were transfected with 0.5 μg plasmids using Lipofectamine 2000. After 6 h of transfection, the medium was replaced with complete medium, and the cells were cultured for another 24 h.

2.2 | Isolation of fPMVs, and Characterization

The transfected rBMSCs and control rBMSCs were harvested, digested with 0.25% trypsin (Beyotime, Shanghai, China), and centrifuged at 1000 rpm for 5 min. Then, the cells and 5 mL medium were first mechanically extruded with a 3 μm-diameter filter, and then mechanically extruded with a 1 μm-diameter filter, repeated for 3 times. The collected filtrate was fPMVs containing VSVG protein and fPMVs. After centrifugation at

10000 g for 5 min, the upper culture medium was removed, and about 500 μL of fPMVs solution was retained. Additionally, the morphology and ultrastructure of the obtained fPMVs were observed under a transmission electron microscopy (TEM, JEOL LTD, Peabody, MA, USA) as previously described [25]. Briefly, the prepared fPMVs (20 μL) were added to the copper screen for absorption for 10 min, and then the excess droplets were removed with filter paper strips. Afterwards, 2% phosphotungstic acid solution (20 μL) was added, and after standing for 5 min, the excess droplets were removed. After drying under an incandescent lamp, the images were photographed under a TEM.

2.3 | Co-Culture of fPMVs and rBMSCs or H9c2 Cells

For the co-culture of fPMVs and rBMSCs, rBMSCs co-transfected with pLP-VSVG and pDSRed-Express2-N1 plasmids or co-transfected with pLP-VSVG and pMito-GFP plasmids cultured for 48 h were used to isolate the fPMVs labeling with red fluorescence or green fluorescence. The rBMSCs were seeded into a 24-well plate overnight, and after washing, the fPMVs labeling with red fluorescence or green fluorescence (10 μg/mL) were added to the cells. After co-culturing for 24 h, the cells were fixed with 4% paraformaldehyde for 20 min, and sealed with Mounting Medium containing DAPI. Finally, the cell images were observed and taken under a laser scanning confocal microscope.

For the co-culture of fPMVs and H9c2 cells, 50 nM MitoTracker Green (KeyGEN BioTECH, Jiangsu, China) was added to fPMVs, and after incubating at 37°C for 30 min, the labeled fPMVs (green fluorescence) were centrifuged at 12000 g at 4°C for 30 min. The sediments were resuspended with 200 μL PBS. The H9c2 cells were seeded into a 24-well plate overnight and were added with the labeled fPMVs (20 μg/mL). After co-culturing for 24 h, the cells were washed with PBS, and then 50 nM MitoTracker Red (KeyGEN BioTECH) was added to the cells. After incubating at 37°C for 30 min, the cells were fixed, sealed, and photographed by a laser scanning confocal microscope.

2.4 | Cell Viability and Apoptosis Assays

To construct an in vitro cardiomyocyte HR injury model, different concentrations of $CoCl_2$ (400, 600, and 800 μM) were firstly used to treat H9c2 cells, and then cell apoptosis, inflammatory cytokines, and mitochondrial function-related indexes were measured to select the optimal concentration of $CoCl_2$. In brief, H9c2 cells were inoculated to a 96-well plate at a density of 5×10^3 and cultured overnight. On the next day, the cells were firstly maintained in low-glucose (1 g/L) serum-free DMEM medium with different concentrations of $CoCl_2$ (final concentration at 0, 400, 600, and 800 μM) at 37°C for 12 h; and then were cultured in high-glucose (4.5 g/L) normal medium for 12 h. After that, different concentrations of fPMVs containing VSVG protein (10, 20, and 50 μg/mL) were added to the cells. After being cultured for another 24 h, each well was added with 10 μL cell counting kit-8 (CCK-8, Beyotime Biotechnology, Shanghai, China). After 2 h of incubation, the values of optical density at 450 nm were measured using a microplate reader (Thermo Fisher Scientific, USA).

Based on the manufacturer's protocols, the apoptosis of H9c2 cells with different treatments was determined using an Annexin V-FITC apoptosis assay kit (Beyotime Biotechnology). The harvested cells were centrifuged at 1000 rpm for 5 min and then resuspended with Annexin V-FITC binding solution. Afterwards, 5 μL Annexin V-FITC and 5 μL propidium iodide (PI) were added. After incubating at 25°C for 20 min in the dark, the cell images were acquired by a flow cytometry (Becton, Dickinson and Company, NJ, USA), and CellQuest software (Becton, Dickinson and Company) was employed to calculate the total cell apoptosis.

2.5 | Determination of Reactive Oxygen Species (ROS)

To analyze ROS levels in the cells, flow cytometry was used with a ROS assay kit (chemical fluorescence method) (Nanjing Jiancheng Bioengineering Institute, Nanjing, China) following the manufacturer's instructions. The H9c2 cells with different treatments were washed with PBS twice and centrifuged at 1000 rpm for 5 min. The sediments were resuspended with PBS containing 10 μM DCFH-DA probes and cultured at 37°C for 60 min. The DCFH-DA-labeled cells were centrifuged at 1000 rpm for 5 min, and the supernatant was removed. After washing with PBS twice, the sediments were collected and resuspended with PBS for flow cytometry detection. The best excitation wavelength was 488 nm, and the best emission wavelength was 525 nm.

For analyzing ROS levels in cell mitochondria, the MitoSOX kit (Thermo Fisher Scientific) was used. The H9c2 cells with different treatments were added to MitoSOX at a final concentration of 5 μmol/L. After incubating at 37°C in the dark for 30 min, the excess staining solution was removed, and the cells were washed with PBS twice. After being resuspended with 1 mL PBS, the cell pictures were observed under a laser scanning confocal microscope.

2.6 | Enzyme-Linked Immunosorbent Assay (ELISA)

The H9c2 cells with different treatments were employed to isolate mitochondria using a Mitochondrial Isolation and Protein Extraction Kit (Proteintech, Wuhan, China) according to the recommendations of the manufacturer. Then, the contents of tumor necrosis factor (TNF)-α and interleukin (IL)-1β in cells and cell mitochondria were measured using the rat TNF-α ELISA kit (Meimian Biotech, Wuhan, China) and rat IL-1β ELISA kit (Meimian Biotech), respectively. Additionally, the adenosine triphosphate (ATP) levels and the concentrations of mitochondrial respiratory chain complex IV (MRCC IV) in cell mitochondria were respectively examined by ATP assay kit (Beyotime Biotechnology) and rat MRCC IV ELISA kit (Meimian Biotech) based on their corresponding manufacturer's instructions.

2.7 | Quantitative Real-Time PCR (qPCR)

The cells with different treatment or fPMVs were used to isolate total DNA using a gDNA extraction kit (Servicebio, Wuhan, China) based on the manufacturer's protocols, and then the isolated DNA was applied for qPCR. The reaction system of qPCR contained 10 μL PerfectStart Green qPCR SuperMix (TransGen Biotech, Beijing, China), 0.4 μL forward primer (10 μM), 0.4 μL reverse primer (10 μM), 2 μg DNA, and sterile water (up to 20 μL). The reaction was initiated at 95°C for 30 s, followed by a total of 40 cycles of 95°C for 5 s and 95°C for 30 s, as well as 95°C for 15 s, 60°C for 60 s, and 95°C for 15 s. The sequences of all primers were shown in Table 1, and *MT-CO3* (for mitochondrial genes) or *β-globin* was used as a reference gene. The expression of relevant genes was calculated by the $2^{-\Delta\Delta Ct}$ method.

2.8 | Western Blot

Total proteins were extracted from the cells with different treatments or different fPMVs using RIPA lysis buffer (Beyotime Biotechnology), as well as were qualified and quantified by 2% agarose gel electrophoresis and a BCA assay kit (Beyotime Biotechnology). After that, the protein samples (20 μg) were segregated by 10% SDS-PAGE and transferred to PVDF membranes. After blocking with 5% skim milk at 37°C for 1 h, the membranes were respectively incubated with the primary antibodies, including anti-CD81 antibody (1:1000, Abcam, USA), anti-eEF2 antibody (1: 1200, Sangon Biotech, Shanghai, China), anti-MTCO1 antibody (1: 1000, BOSTER Biological Technology Co. Ltd., Wuhan, China), anti-TOMM20 antibody (1: 1000, Wanlei Bio, Shenyang, China), anti-VSVG antibody (1: 1000, BOSTER Biological Technology Co. Ltd.), and anti-β-actin antibody (1: 20000, Proteintech), at 4°C overnight. Then, the membranes were incubated with goat anti-mouse IgG (H + L)-HRP (1: 5000, Jackson ImmunoResearch) or goat anti-rabbit IgG (H + L)-HRP (1: 5000, Jackson ImmunoResearch) at 37°C for 2 h. Eventually, the Millipore electrochemiluminescence ECL system (Beyotime Biotechnology) was employed to visualize the protein bands.

TABLE 1 | The sequences of all primers.

Primer	Sequences (5′-3′)
MT-ND4-rF	AGCTCCAATTGCAGGCTCTA
MT-ND4-rR	CTGTTTGGCGTAGGCAGATT
HDAC1-rF	CTGGGGACCTACGGGATATT
HDAC1-rR	CACTGCACTAGGCTGGAACA
ACTB-rF	GTCGTACCACTGGCATTGTG
ACTB-rR	CTCTCAGCTGTGGTGGTGAA
MT-CO3-rF	AGCCCATGACCACTAACAGG
MT-CO3-rR	TGGCCTTGGTATGTTCCTTC
MT-ND1-F	CCTTCCTATTTCTCGCTACACCTA
MT-ND1-R	GCGAGGATAAACAGTATCCCTAGA
β-globin-F	ACCTGACTCCTGATGAGAAGAATG
β-globin-R	CAAAGGAGTCAAAGAACCTCTGG

2.9 | Statistical Analysis

Data were expressed as mean ± standard deviation. Statistical analysis was performed in SPSS software, and GraphPad Prism 5.0 (GraphPad Software, San Diego, CA, USA) was employed for plotting. For comparison between the two groups, Student's *t* test was used, as well as one-way analysis of variance followed by the Bonferroni Method was applied for the comparison among more than two groups. $p < 0.05$ was regarded as statistically significant.

3 | Results

3.1 | Characterization and Uptake of fPMVs

In order to obtain the fPMVs containing VSVG protein, rBMSCs were transfected with pLP-VSVG plasmids, and then fPMVs were isolated from rBMSCs and rBMSCs with VSVG overexpression. The representative images of rBMSCs and rBMSCs with VSVG overexpression were shown in Figure 1A. TEM results showed that fPMVs isolated from the rBMSCs with VSVG overexpression exhibited a nearly round morphology with a diameter of about 500 nm (big) or 250 nm (small) (Figure 1B).

Further to observe whether fPMVs can enter rBMSCs, fPMVs were labeled with red fluorescence and then co-cultured with rBMSCs. After 24 h of co-incubation, red fluorescence was shown in rBMSCs (Figure 1C), which indicated that fPMVs could be taken up by rBMSCs. In addition, MitoTracker Green was used to label the mitochondria of fPMVs (green fluorescence), rBMSCs were stained red, and the nuclei were stained blue by DAPI. It was found that most rBMSCs exhibited intracellular fluorescence, and the labeled fPMVs (green) were localized in the cytoplasm after co-culture (Figure 1D). These results suggested that fPMVs or the mitochondria of fPMVs could enter into the rBMSCs.

After that, to further characterize the fPMVs and the mitochondrial functions of fPMVs, the expression of nuclear genes (*ACTB*, and *HDAC1*), mitochondrial gene/protein (*MT-ND4*, MTCO1, and TOMM20), VSVG, membrane protein CD81, and cytosolic protein eEF2 were determined in different rBMSCs or fPMVs by qPCR and western blot. No significant difference was found in the *MT-ND4* expression between the rBMSCs and rBMSCs with VSVG overexpression, as well as between the fPMVs and fPMVs with VSVG overexpression ($p > 0.05$, Figure 2A,B). For *ACTB* and *HDAC1*, their expression was significantly increased in the rBMSCs with VSVG overexpression or fPMVs with VSVG overexpression compared to the control rBMSCs or fPMVs ($p < 0.05$, Figure 2A,B). Western blot showed that the protein expression of VSVG, CD81, MTCO1, and TOMM20 was evidently up-regulated, while eEF2 protein expression was markedly down-regulated in the rBMSCs with VSVG overexpression relative to the control rBMSCs ($p < 0.05$, Figure 2C). The tendency of the VSVG, CD81, eEF2, MTCO1, and TOMM20 protein expression in the different fPMVs was similar to that in the different rBMSCs (Figure 2D). These findings indicated that fPMVs containing VSVG protein

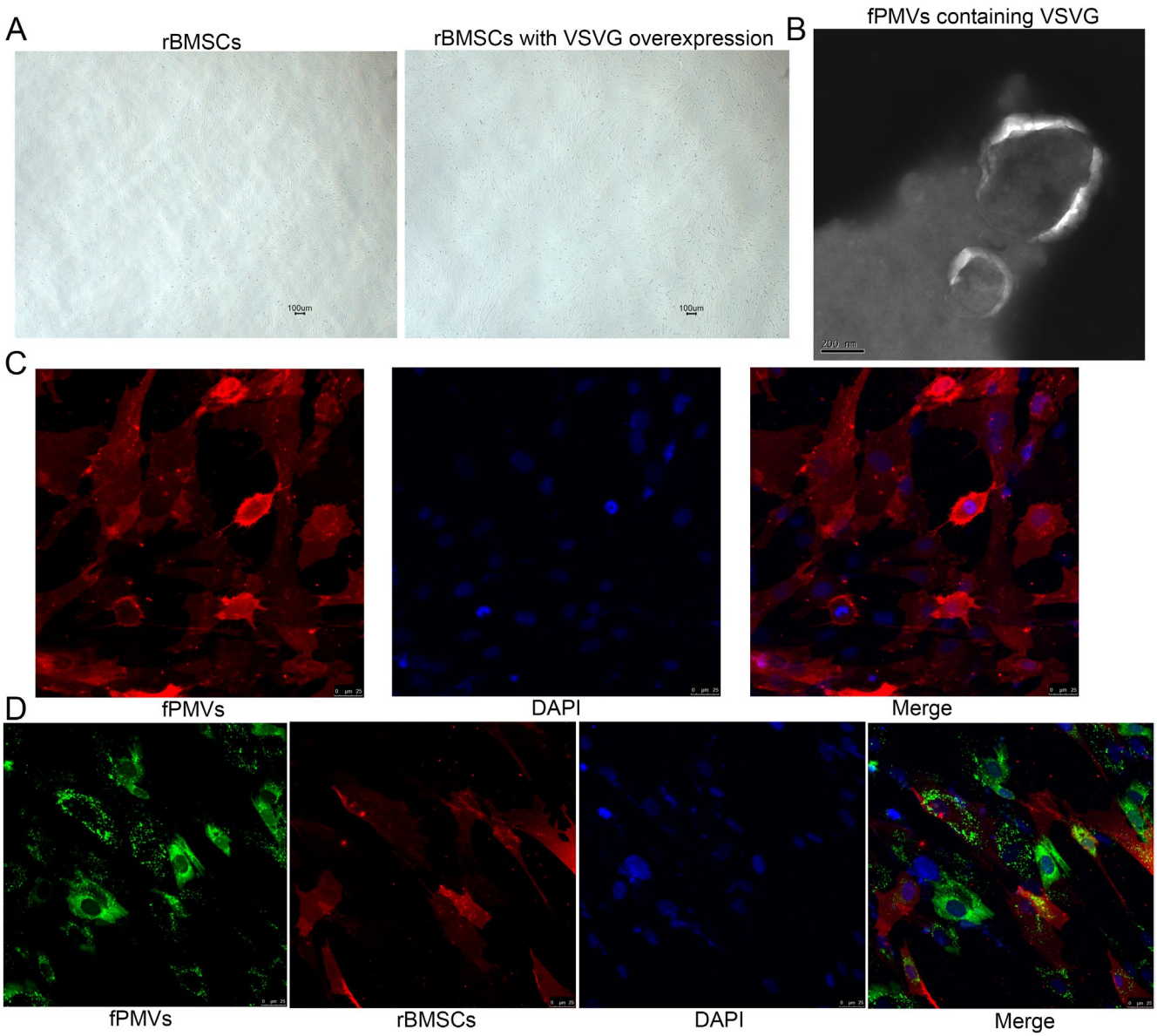

FIGURE 1 | Characterization and uptake of fusogenic plasma membrane vesicles (fPMVs) in rat bone marrow mesenchymal stem cells (rBMSCs). (A) The representative images of rBMSCs and rBMSCs with VSVG overexpression. (B) The morphology of fPMVs visualized using a transmission electron microscopy. (C) fPMSVs were labeled with red fluorescence, and fPMVs could be taken up by rBMSCs. (D) MitoTracker Green was used to label mitochondria of fPMVs (green fluorescence), rBMSCs were stained red, and nucleus were stained blue by DAPI. Mitochondria of fPMVs could enter into the rBMSCs.

were successfully isolated, and the mitochondrial functions may be enhanced after VSVG overexpression.

3.2 | Select the Optimal Concentration of $CoCl_2$ in H9c2 Cells

Compared to the control H9c2 cells, $CoCl_2$ treatment significantly induced cell apoptosis ($p < 0.05$), and the total apoptosis percentage was gradually increased with the increase of $CoCl_2$ concentration (Figure 3A). Then, the levels of inflammatory cytokines in the H9c2 cells with different treatments were examined. It was found that there were no significant differences in the contents of TNF-α and IL-1β between the control and 400 μM $CoCl_2$-treated cells ($p > 0.05$, Figure 3B,C). However, 600 and 800 μM $CoCl_2$ significantly increased the TNF-α and IL-1β contents in comparison with the control H9c2 cells ($p < 0.05$, Figure 3B,C).

Additionally, the ROS levels were significantly higher in the $CoCl_2$-treated cells than those in the control cells ($p < 0.05$), and were gradually enhanced with the increasing concentrations of $CoCl_2$ (Figure 4A). The trend of TNF-α and IL-1β contents in the cellular mitochondria with different treatments was in accordance with that in the H9c2 cells (Figure 4B,C). Finally, the expression of *MT-ND1* was determined by qPCR. It was obvious that 400 μM $CoCl_2$ treatment did not evidently change the expression of *MT-ND1* ($p > 0.05$); whereas the expression

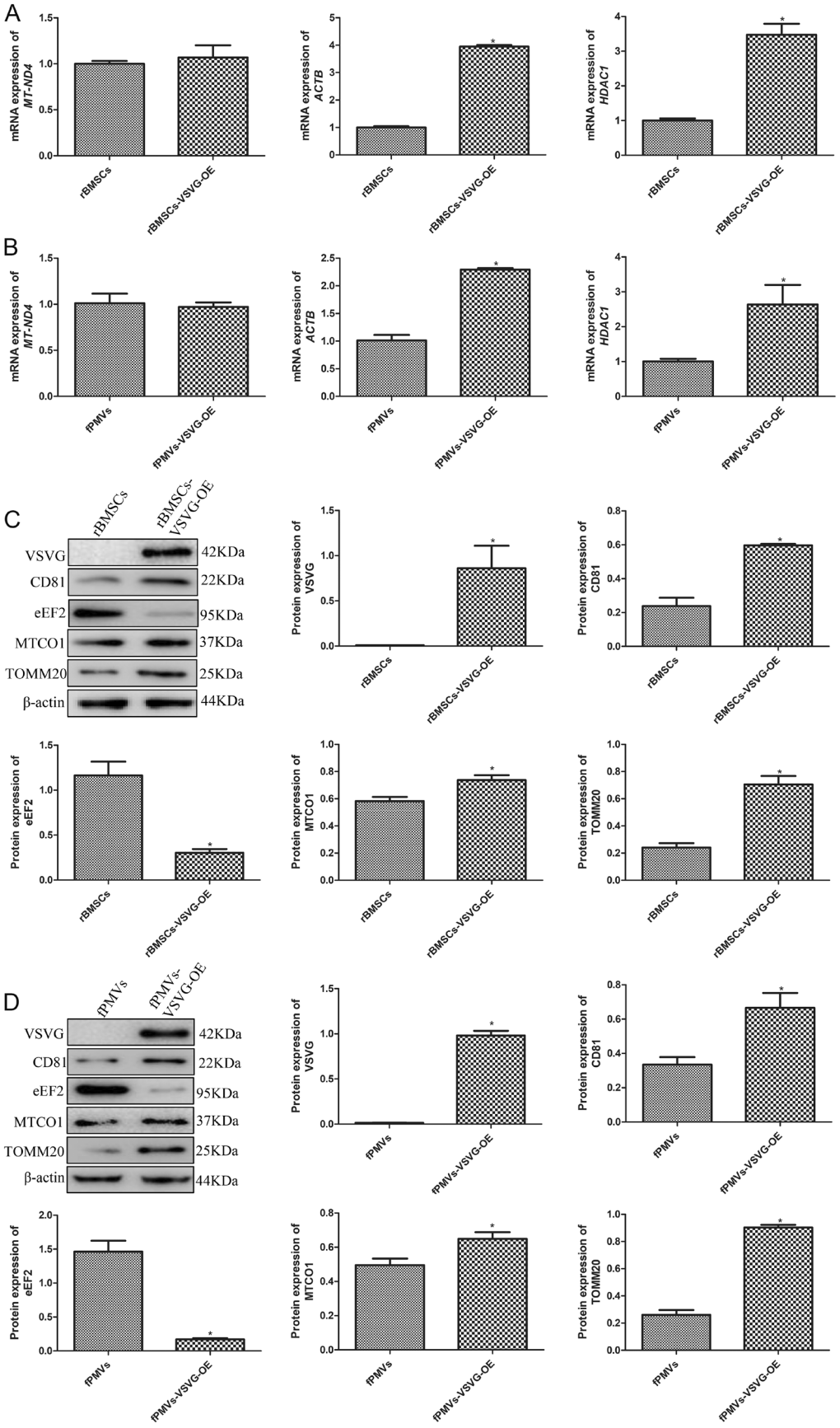

FIGURE 2 | Legend on next page.

FIGURE 2 | Expression of mitochondrial function-related genes/proteins and fPMVs-related proteins determined by quantitative real-time PCR (qPCR) or western blot. (A) The expression of *MT-ND4*, *ACTB*, and *HDAC1* in the rBMSCs and rBMSCs with VSVG overexpression. *$p < 0.05$, vs. rBMSCs. (B) The expression of *MT-ND4*, *ACTB*, and *HDAC1* in the fPMVs and fPMVs with VSVG overexpression. *$p < 0.05$, vs. fPMVs. (C) The protein expression of VSVG, CD81, eEF2, MTCO1, and TOMM20 in the rBMSCs and rBMSCs with VSVG overexpression. *$p < 0.05$, vs. rBMSCs. (D) The protein expression of VSVG, CD81, eEF2, MTCO1, and TOMM20 in the fPMVs and fPMVs with VSVG overexpression. *$p < 0.05$, vs. fPMVs.

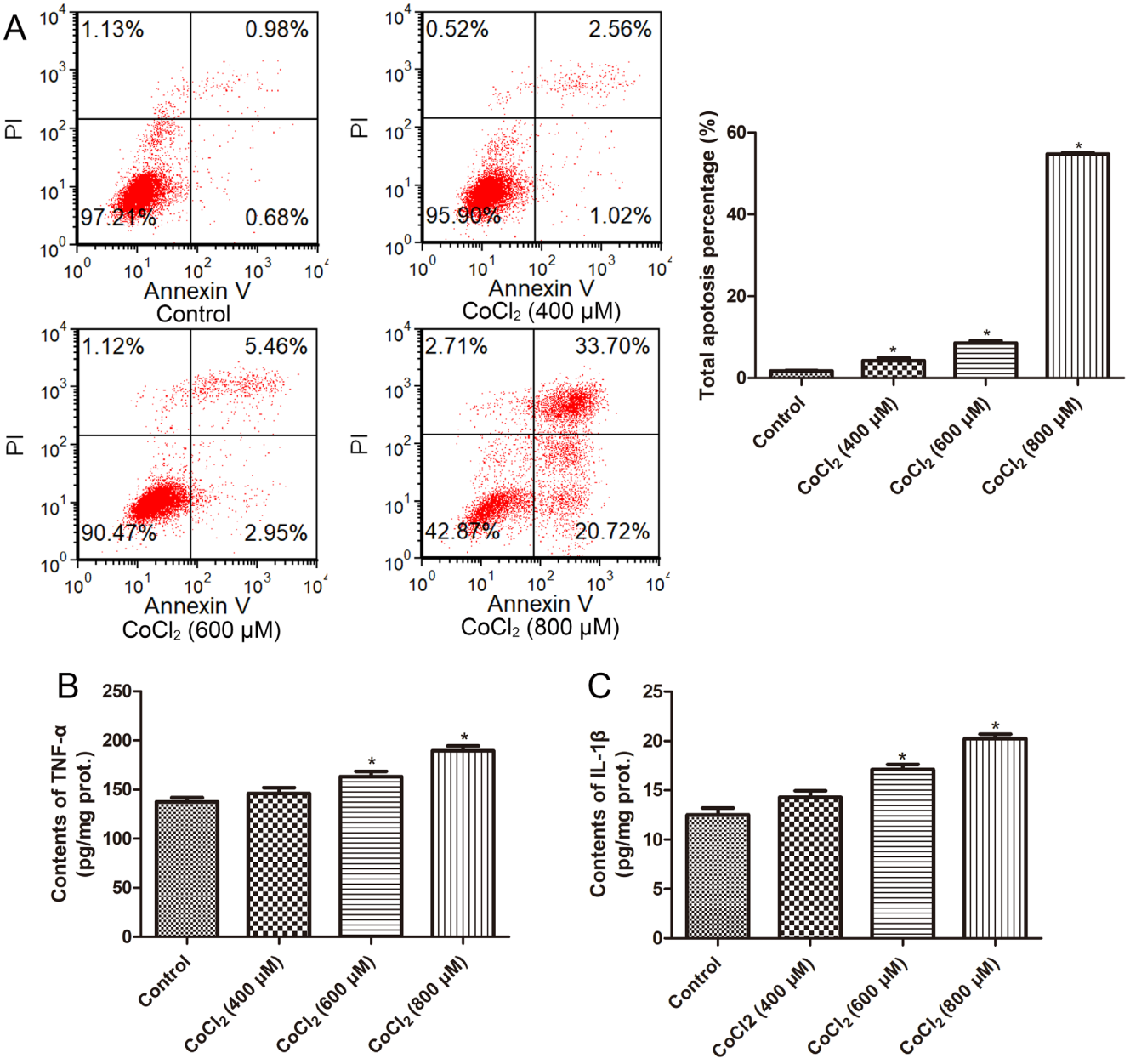

FIGURE 3 | Effects of different concentrations of $CoCl_2$ on the apoptosis of H9c2 cells, and the levels of inflammatory cytokines in cells. (A) The cell apoptosis percentage in different groups using a flow cytometry. (B) The contents of TNF-α in the H9c2 cells with different treatments. (C) The contents of IL-1β in the H9c2 cells with different treatments. *$p < 0.05$, vs. control.

of *MT-ND1* in the 600 and 800 μM $CoCl_2$-treated cells was significantly lower than that in the control H9c2 cells ($p < 0.05$, Figure 4D). Therefore, under hypoxia conditions, the apoptosis of H9c2 cells and inflammatory levels could be enhanced, while mitochondrial function may be decreased. In the subsequent experiments, we chose 600 μM $CoCl_2$ to induce a hypoxia environment.

3.3 | Uptake of fPMVs by H9c2 Cells

Further to investigate the effects of fPMVs containing VSVG protein on cardiomyocyte HR injury, we firstly need to confirm whether fPMVs can be taken up by H9C2 cells. The mitochondria of fPMVs were labeled with green fluorescence, H9c2 cells were stained red, and the nucleus was stained blue by DAPI. It

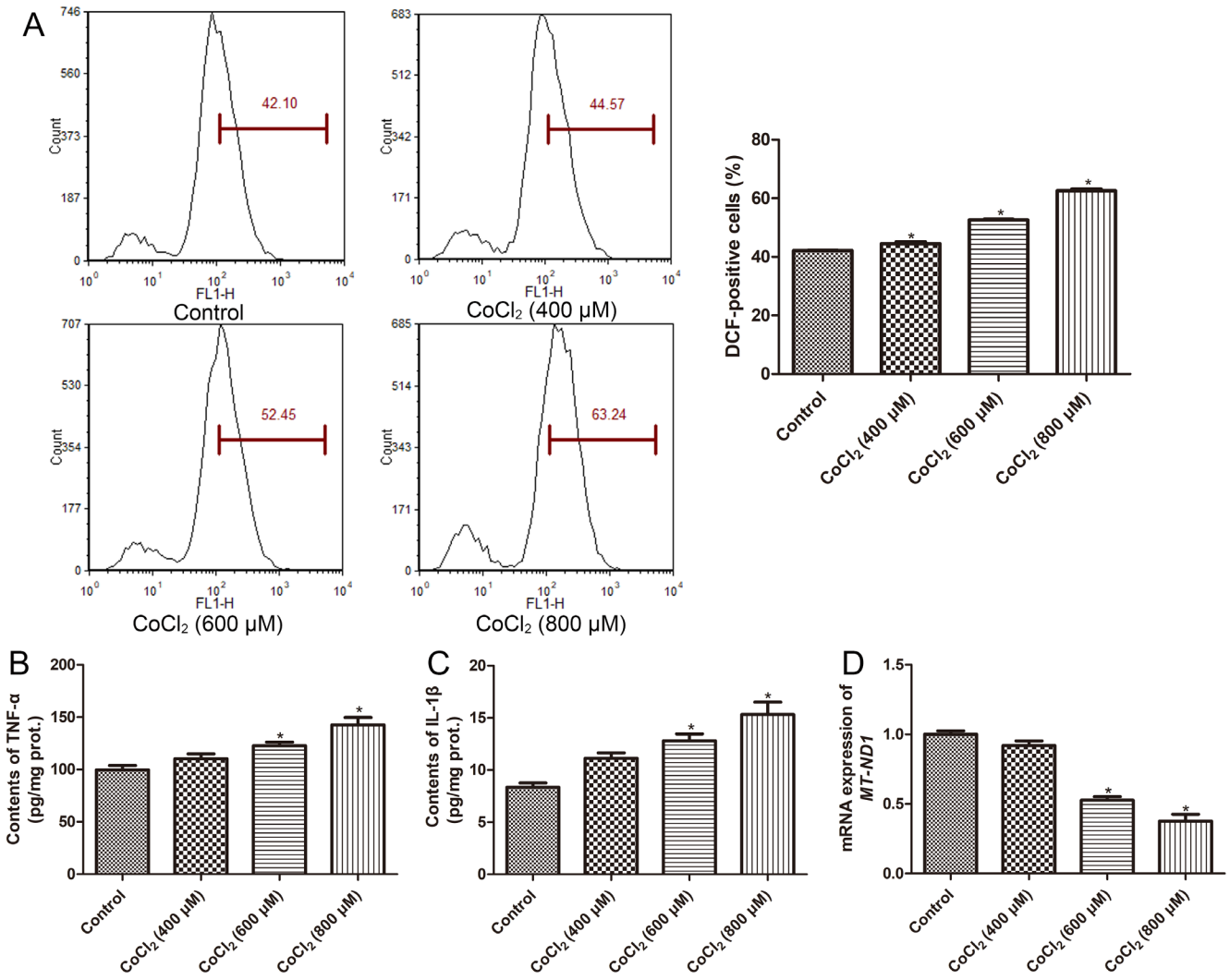

FIGURE 4 | Effects of different concentrations of $CoCl_2$ on the levels of reactive oxygen species (ROS), *MT-ND1* and inflammatory cytokines in cellular mitochondria. (A) The levels of ROS in H9c2 cells treated with different concentrations of $CoCl_2$. (B) The contents of TNF-α in the cellular mitochondria with different concentrations of $CoCl_2$ treatments. (C) The contents of IL-1β in the cellular mitochondria with different concentrations of $CoCl_2$ treatments. (D) The expression of *MT-ND1* in the H9c2 cells treated with different concentrations of $CoCl_2$. $^*p < 0.05$, vs. control.

was found that most H9c2 cells showed intracellular fluorescence, and the labeled fPMVs (green) were localized in the cytoplasm after co-culture (Figure 5A). These indicated that fPMVs could carry mitochondria into H9c2 cells.

3.4 | Effects of fPMVs on the Growth of H9c2 Cells Induced by HR

CCK-8 was employed to further study the effects of fPMVs on the viability of H9c2 cells induced by HR. It is clear that the cell viability in the HR-treated cells was significantly inhibited compared to the control cells ($p < 0.05$, Figure 5B). Then, different concentrations of fPMVs (10, 20, and 50 μg/mL) were used to treat the HR-induced H9c2 cells, and we observed that there was no significant difference in cell viability between the HR and HR + fPMVs (10 μg/mL) groups ($p > 0.05$). However, 20 and 50 μg/mL fPMVs treatments significantly enhanced the viability of HR-induced H9c2 cells in comparison with the HR-induced H9c2 cells ($p < 0.05$, Figure 5B). Hence, 20 μg/mL fPMVs were selected for subsequent study, as well as fPMVs containing VSVG protein could promote the growth of HR-induced H9c2 cells.

3.5 | Effects of fPMVs on the Mitochondrial Functions of H9c2 Cells Induced by HR

To explore whether fPMVs affect cell viability through mitochondria transfer, the *MT-ND1* expression, the levels of inflammatory cytokines, ATP, MRCC IV, and ROS in cellular mitochondria were determined. It was observed that the expression of *MT-ND1* was significantly increased in the HR + fPMVs groups compared to the HR group ($p < 0.05$, Figure 6A). Compared to the control cells, HR treatment significantly increased the contents of TNF-α and IL-1β ($p < 0.05$); while fPMVs evidently restored their contents to a similar level as the control H9c2 cells ($p > 0.05$, Figure 6B,C). The ATP contents in the control, HR, and HR + fPMVs groups were respectively 0.199 ± 0.024, 0.124 ± 0.012, and 0.178 ± 0.017 μmol/mg protein, which indicated

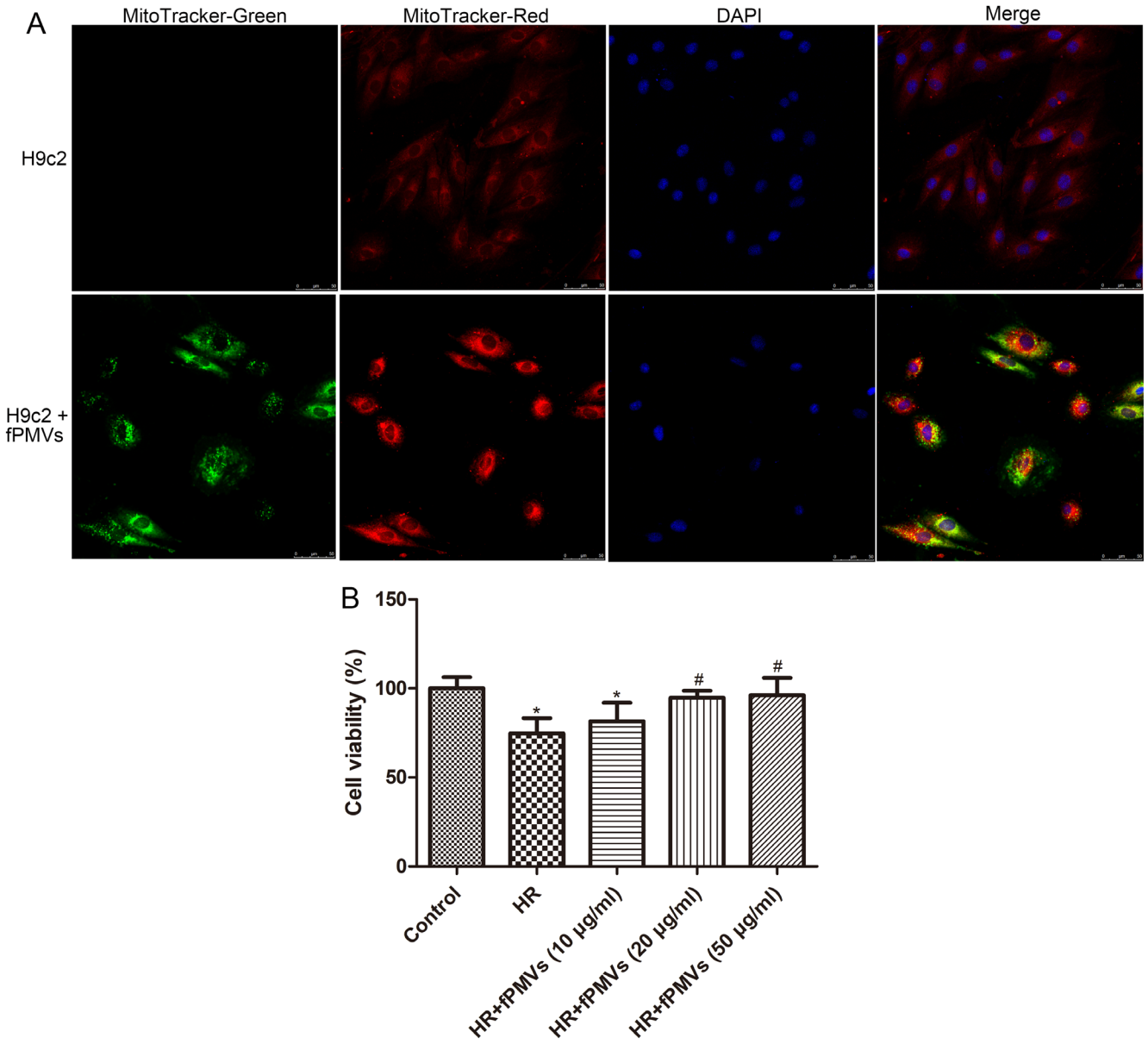

FIGURE 5 | Effects of fPMVs on the growth of H9c2 cells induced by hypoxia reoxygenation (HR). (A) The mitochondria of fPMVs were labeled green fluorescence, and fPMVs could carry mitochondria into H9c2 cells. (B) The cell viability of HR-induced H9c2 cells treated with different concentrations of fPMVs. $^{*}p < 0.05$, vs. control, $^{\#}p < 0.05$, vs. HR.

that HR significantly decreased the ATP content compared to the control cells ($p < 0.05$), whereas fPMVs evidently increased its contents induced by HR ($p < 0.05$, Figure 6D). Additionally, the contents of MRCC IV in the control, HR, and HR + fPMVs groups were 7.644 ± 0.271, 0.808 ± 0.092, and 2.123 ± 0.454 pg/μg protein, respectively. These showed that the MRCC IV contents were significantly lower in the HR group than in the control group ($p < 0.05$), but were remarkably higher in the HR + fPMVs group than in the HR group ($p < 0.05$, Figure 6E). The results of confocal microscopy exhibited that the red fluorescence in the HR-induced cells was stronger than that in the control cells; while fPMVs weakened the red fluorescence caused by HR (Figure 6F). These outcomes implied that fPMVs could reduce the ROS levels caused by HR in cellular mitochondria.

4 | Discussion

Myocardial ischemia–reperfusion injury is an inevitable risk event of acute myocardial infarction, and recently, the incidence and mortality of myocardial HR injury have gradually risen [5, 26]. BMSCs have multi-prong capabilities, including angiogenesis, promoting wound healing, anti-inflammatory effects, immune regulation, and antioxidant properties [27], and BMSCs-derived fPMVs may have typical and significant properties of functional BMSCs. In this study, rBMSCs with VSVG overexpression were successfully established, and fPMVs containing VSVG protein were prepared. It was found that fPMVs and their mitochondria could be taken up by rBMSCs, as well as in the fPMVs containing VSVG protein, *ACTB*, *HDAC1*, VSVG,

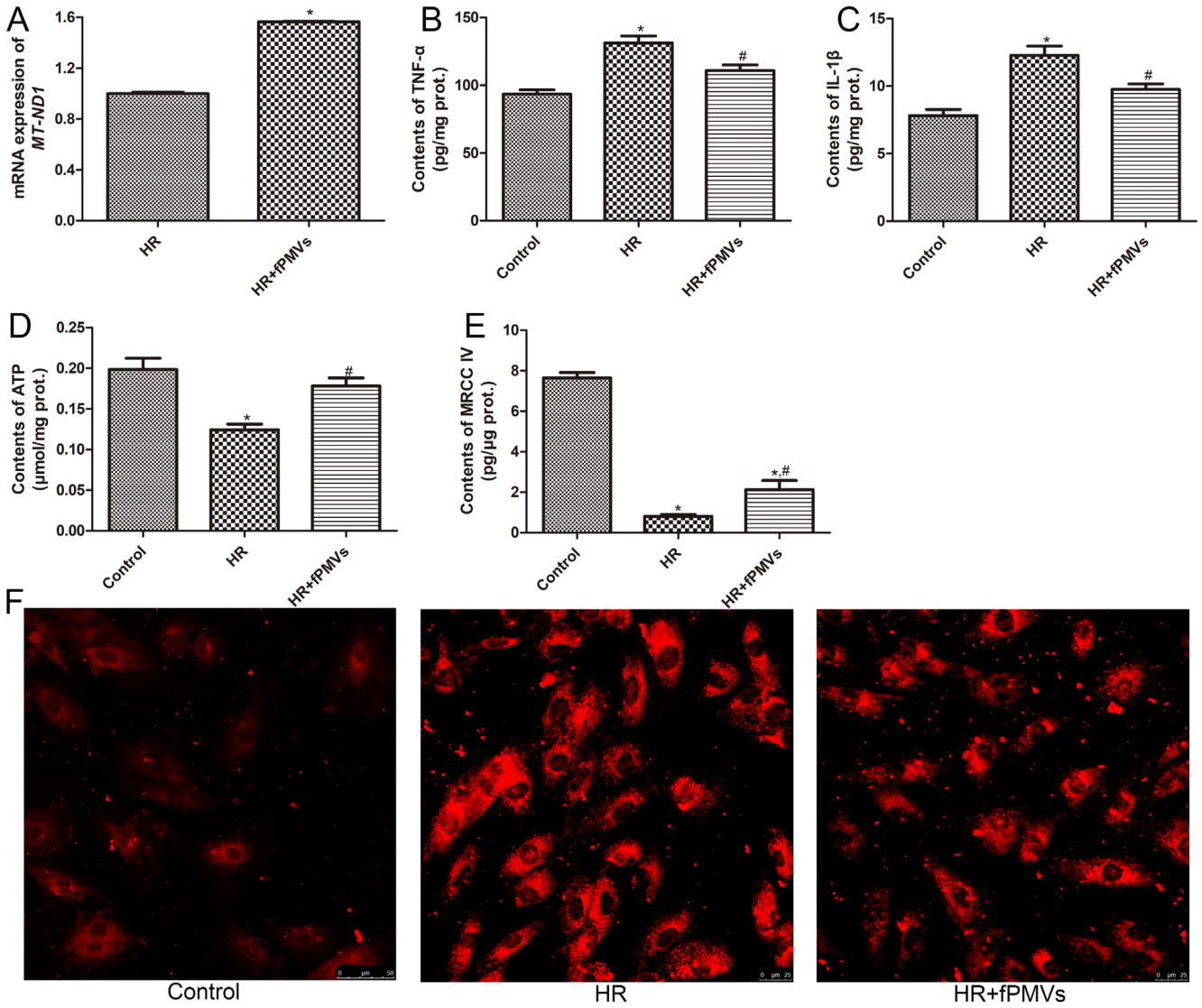

FIGURE 6 | Effects of fPMVs on the mitochondrial functions of H9c2 cells induced by HR. (A) The expression of *MT-ND1* in the HR-induced H9c2 cells treated with fPMVs. $^{*}p < 0.05$, vs. control. The contents of TNF-α (B), IL-1β (C), ATP (D), and MRCC IV (E) in the cellular mitochondria with different treatments. (F) The ROS levels in the cellular mitochondria with different treatments under a laser scanning confocal microscope. $^{*}p < 0.05$, vs. control, $^{\#}p < 0.05$, vs. HR.

CD81, MTCO1, and TOMM20 were up-regulated, while eEF2 was down-regulated.

ACTB is a highly conserved cytoskeletal structural protein and has been considered a common housekeeping gene for many years [28]. A previous study has demonstrated that ACTB can interact with p53 and negatively regulate p53 nuclear input through protein–protein interactions [29]. HDAC1 is an inhibitor of epigenome gene transcription and is involved in DNA damage and cell cycle regulation. It was found that HDAC1 could play a crucial role in ischemia reperfusion–induced neuroinflammation and blood–brain barrier damage, thereby implying its potential as a therapeutic target [30]. The VSVG protein not only produces stable, high titer lentiviral vectors with broad cell affinity but also produces virus-like particles when it is ectopically expressed in a variety of eukaryotic cells [31]. In addition, VSVG has been modified to target specific cell types and has become one of the most widely used platforms for biomedical applications [32]. Wang et al. [31] demonstrated that engineered lentiviral envelope VSVG could target delivery of IDOL-shRNA to the liver, thereby ameliorating hypercholesterolemia and atherosclerosis. It is known that eEF2 is a cytosolic protein and is at least partially involved in peptide chain elongation in protein synthesis under multiple stimuli. Moreover, the antidepressant effect of fluoxetine could be involved in HDAC1-eEF2-related neuroinflammation and synaptogenesis [33]. CD81, a membrane protein, has a major role in the regulation of cellular interactions and cell transport, as well as has been confirmed as a marker for EVs [34]. MTCO1 is a key molecule of mitochondria and TOMM20 is a structural protein of mitochondria that is responsible for the recognition and translocation of mitochondrial proteins from the cytosol [35]. Combined with our results, it can be inferred that the isolated fPMVs may contain cytoplasm, plasma membrane, VSVG protein, and organelles, as well as may deliver cytoplasmic proteins and mitochondria to target cells.

Further to explore the effects of the isolated fPMVs on the myocardial injury, we constructed a cardiomyocyte injury model by

HR, and then treated with fPMVs. It was obvious that fPMVs could carry mitochondria into H9c2 cells, and HR treatment could significantly inhibit viability and induce apoptosis of H9c2 cells; as well as significantly increase the contents of TNF-α and IL-1β, and ROS levels both in cells and cellular mitochondria, while evidently reducing the levels of ATP, MRCC IV, and *MT-ND1*. However, fPVMs could remarkably reverse the changes in these indexes caused by HR. Myocardial ischemia–reperfusion injury caused by HR is a complex pathophysiological process. When calcium is overloaded, the mitochondrial permeability transition pore opens, and the production of ROS increases, leading to mitochondrial dysfunction and cell death, as well as during the process of ischemia–reperfusion, many harmful inflammatory cytokines are released, for example, IL-6, IL-1β, and TNF-α [4]. Mitochondria have many functions that support cell growth, division, and apoptosis; as well as important to mitochondrial function is the protein translocation system, which requires many proteins to function properly [36]. A previous study has reported that after HR, the viability of H9c2 cells was decreased, and the release of lactic dehydrogenase and cell apoptosis were increased, accompanied by a higher level of calcium [37], which were in accordance with our outcomes.

ATP is the most common and important energy molecule in the cell. In order to maintain heart function, cardiomyocytes require a constant supply of energy, mostly in the form of ATP [38]. Zhang et al. [39] demonstrated that ATP contents in the HR-induced H9c2 cells were significantly decreased, but the pretreatment of Shen Yuan Dan could enhance the ATP contents and have a protective function in cardiomyocyte H/R injury by regulating mitochondrial mass. Furthermore, most of the cellular ATP used in the heart (> 90%) is produced by oxidative phosphorylation of mitochondria, so to study the downstream factors of fMVPs affecting ATP synthesis, we detected the expression of *MT-ND1* and the contents of MRCC IV. MT-ND1, located in the mitochondrial membrane, provides MRCC I with NADH dehydrogenase activity and is involved in mitochondrial electron transport and assembly of MRCC I [40]. MT-ND1 plays an important role in maintaining the normal physiological function of the body, and its up-regulation or ectopic expression can improve the disease phenotype [40]. MRCC IV is another essential component of the oxidative respiratory chain, is crucial for the generation of ATP in most eukaryotic cells [41]. An anterior research demonstrated that the ATP content, *TFAM*, *MT-ND1*, and *MT-CO1* expression were all decreased in the fast-pacing cardiomyocytes; whereas the recovery of TFAM could increase the ATP content by up-regulating *MT-ND1* and *MT-CO1* in fast pacing cardiomyocytes, thus improving atrial fibrillation [38]. Mitochondria are the primary sites of ROS production, and it has been reported that ROS produced within mitochondria are special drivers for HR damage, including induction of mitochondrial permeability transition or oxidative damage of mitochondrial structures and molecules [42]. TNF-α and IL-1β are two pro-inflammatory cytokines and are observed to be increased in the HR-induced myocardial ischemia–reperfusion injury [43]. Cen et al. [44] elaborated that HR significantly increased the production of ROS and pro-inflammatory cytokines; while APPL overexpression could suppress the production of ROS and pro-inflammatory cytokines (TNF-α, MCP-1, and IL-1β), thus relieve HR-induced myocardial damage. Another study also confirmed the increased levels of ROS, TNF-α, and IL-1β in H9c2 cells after HR, but paeonol pretreatment could mitigate HR-caused H9c2 injury through inhibiting ROS levels and down-regulating TNF-α and IL-1β contents [45]. Taken together, we speculate that fPMVs may improve myocardial injury caused by HR through regulating cellular mitochondrial function (ROS, ATP, MRCC IV, and *MT-ND1*) and inflammatory levels (TNF-α and IL-1β).

In conclusion, rBMSCs-derived fPMVs containing VSVG may exert protective effects on ischemia reperfusion myocardial injury. The possible protection mechanisms are related to the mitochondrial transfer of fPMVs, the inhibited inflammatory response by decreasing TNF-α and IL-1β levels, and regulation of cellular mitochondrial functions. However, our work is a preliminary study, and the application of fPMVs in vivo needs to be investigated in the future. Our findings broaden our understanding of rBMSCs-derived fPMVs in disease therapy and lay the foundation for rBMSCS-derived fPMVs as a novel stem cell therapeutic strategy for myocardial injury.

Author Contributions

Conception and design of the research: Xin Liu and Hong Bian; acquisition of data: Xin Liu, Tingyuan Zhou, Chunjuan Zhao, and Hong Bian; analysis and interpretation of data: Tingyuan Zhou and Chunjuan Zhao; statistical analysis: Tingyuan Zhou and Chunjuan Zhao; Obtaining funding: Xin Liu and Hong Bian; drafting the manuscript: Xin Liu and Hong Bian; revision of manuscript for important intellectual content: Xin Liu and Hong Bian. All authors read and approved the final manuscript.

Acknowledgments

The authors have nothing to report.

Ethics Statement

The authors have nothing to report.

Consent

The authors have nothing to report.

Conflicts of Interest

The authors declare no conflicts of interest.

Data Availability Statement

The dataset used and/or analyzed during the current study is available from the corresponding author on a reasonable request.

References

1. A. S. Perry, E. E. Dooley, H. Master, N. L. Spartano, E. L. Brittain, and K. Pettee Gabriel, "Physical Activity Over the Lifecourse and Cardiovascular Disease," *Circulation Research* 132 (2023): 1725–1740.

2. L. A. Kaminsky, C. German, M. Imboden, C. Ozemek, J. E. Peterman, and P. H. Brubaker, "The Importance of Healthy Lifestyle Behaviors in the Prevention of Cardiovascular Disease," *Progress in Cardiovascular Diseases* 70 (2022): 8–15.

3. J. W. O'Sullivan, S. Raghavan, C. Marquez-Luna, et al., "Polygenic Risk Scores for Cardiovascular Disease: A Scientific Statement From the American Heart Association," *Circulation* 146, no. 8 (2022): e93–e118, https://doi.org/10.1161/CIR.0000000000001077.

4. X. Chen, X. Li, W. Zhang, et al., "Activation of AMPK Inhibits Inflammatory Response During Hypoxia and Reoxygenation Through Modulating JNK-Mediated NF-κB Pathway," *Metabolism, Clinical and Experimental* 83 (2018): 256–270.

5. M. Zhou, Y. Yu, X. Luo, et al., "Myocardial Ischemia-Reperfusion Injury: Therapeutics From a Mitochondria-Centric Perspective," *Cardiology* 146 (2021): 781–792.

6. X. Ding, C. Zhu, W. Wang, M. Li, C. Ma, and B. Gao, "SIRT1 Is a Regulator of Autophagy: Implications for the Progression and Treatment of Myocardial Ischemia-Reperfusion," *Pharmacological Research* 199 (2024): 106957.

7. C. Liu, M. Zhang, S. Ye, et al., "Acacetin Protects Myocardial Cells Against Hypoxia-Reoxygenation Injury Through Activation of Autophagy," *Journal of Immunology Research* 2021 (2021): 9979843.

8. J. G. Rurik, H. Aghajanian, and J. A. Epstein, "Immune Cells and Immunotherapy for Cardiac Injury and Repair," *Circulation Research* 128 (2021): 1766–1779.

9. Y. Wang, J. Fang, B. Liu, C. Shao, and Y. Shi, "Reciprocal Regulation of Mesenchymal Stem Cells and Immune Responses," *Cell Stem Cell* 29 (2022): 1515–1530.

10. L. X. Pang, W. W. Cai, Q. Li, et al., "Bone Marrow-Derived Mesenchymal Stem Cells Attenuate Myocardial Ischemia-Reperfusion Injury via Upregulation of Splenic Regulatory T Cells," *BMC Cardiovascular Disorders* 21 (2021): 215.

11. Q. Chen, Y. Liu, X. Ding, et al., "Bone Marrow Mesenchymal Stem Cell-Secreted Exosomes Carrying microRNA-125b Protect Against Myocardial Ischemia Reperfusion Injury via Targeting SIRT7," *Molecular and Cellular Biochemistry* 465 (2020): 103–114.

12. A. Naji, M. Eitoku, B. Favier, F. Deschaseaux, N. Rouas-Freiss, and N. Suganuma, "Biological Functions of Mesenchymal Stem Cells and Clinical Implications," *Cellular and Molecular Life Sciences* 76 (2019): 3323–3348.

13. T. Lan, M. Luo, and X. Wei, "Mesenchymal Stem/Stromal Cells in Cancer Therapy," *Journal of Hematology & Oncology* 14 (2021): 195.

14. J. Liu, J. Gao, Z. Liang, et al., "Mesenchymal Stem Cells and Their Microenvironment," *Stem Cell Research & Therapy* 13 (2022): 429.

15. A. Walewska, A. Janucik, M. Tynecka, M. Moniuszko, and A. Eljaszewicz, "Mesenchymal Stem Cells Under Epigenetic Control—The Role of Epigenetic Machinery in Fate Decision and Functional Properties," *Cell Death & Disease* 14 (2023): 720.

16. M. J. Lin, S. Li, L. J. Yang, et al., "Plasma Membrane Vesicles of Human Umbilical Cord Mesenchymal Stem Cells Ameliorate Acetaminophen-Induced Damage in HepG2 Cells: A Novel Stem Cell Therapy," *Stem Cell Research & Therapy* 11, no. 1 (2020): 225, https://doi.org/10.1186/s13287-020-01738-z.

17. D. K. Jeppesen, Q. Zhang, J. L. Franklin, and R. J. Coffey, "Extracellular Vesicles and Nanoparticles: Emerging Complexities," *Trends in Cell Biology* 33 (2023): 667–681.

18. F. Urabe, N. Kosaka, K. Ito, T. Kimura, S. Egawa, and T. Ochiya, "Extracellular Vesicles as Biomarkers and Therapeutic Targets for Cancer," *American Journal of Physiology Cell Physiology* 318 (2020): C29–C39.

19. L. Q. Xu, M. J. Lin, Y. P. Li, S. Li, S. J. Chen, and C. J. Wei, "Preparation of Plasma Membrane Vesicles From Bone Marrow Mesenchymal Stem Cells for Potential Cytoplasm Replacement Therapy," *Journal of Visualized Experiments: JoVE* 123 (2017): 55741.

20. P. E. Mangeot, S. Dollet, M. Girard, et al., "Protein Transfer Into Human Cells by VSV-G-Induced Nanovesicles," *Molecular Therapy: The Journal of the American Society of Gene Therapy* 19 (2011): 1656–1666.

21. J. Shoji, Y. Tanihara, T. Uchiyama, and A. Kawai, "Preparation of Virosomes Coated With the Vesicular Stomatitis Virus Glycoprotein as Efficient Gene Transfer Vehicles for Animal Cells," *Microbiology and Immunology* 48 (2004): 163–174.

22. H. P. Lin, D. J. Zheng, Y. P. Li, et al., "Incorporation of VSV-G Produces Fusogenic Plasma Membrane Vesicles Capable of Efficient Transfer of Bioactive Macromolecules and Mitochondria," *Biomedical Microdevices* 18 (2016): 41.

23. Y. S. Gai, Y. H. Ren, Y. Gao, and H. N. Liu, "Astaxanthin Protecting Myocardial Cells From Hypoxia/Reoxygenation Injury by Regulating miR-138/HIF-1α Axis," *European Review for Medical and Pharmacological Sciences* 24 (2020): 7722–7731.

24. H. Sun, S. Ling, D. Zhao, et al., "Ginsenoside re Treatment Attenuates Myocardial Hypoxia/Reoxygenation Injury by Inhibiting HIF-1α Ubiquitination," *Frontiers in Pharmacology* 11 (2020): 532041.

25. L. A. Ovchinnikova, S. S. Terekhov, R. H. Ziganshin, et al., "Reprogramming Extracellular Vesicles for Protein Therapeutics Delivery," *Pharmaceutics* 13 (2021): 768.

26. B. Mi, Q. Li, T. Li, J. Marshall, and J. Sai, "A Network Pharmacology Study on Analgesic Mechanism of Yuanhu-Baizhi Herb Pair," *BMC Complementary Medicine and Therapies* 20 (2020): 284.

27. R. Margiana, A. Markov, A. O. Zekiy, et al., "Clinical Application of Mesenchymal Stem Cell in Regenerative Medicine: A Narrative Review," *Stem Cell Research & Therapy* 13, no. 1 (2022): 366, https://doi.org/10.1186/s13287-022-03054-0.

28. Y. Gu, S. Tang, Z. Wang, et al., "A Pan-Cancer Analysis of the Prognostic and Immunological Role of β-Actin (ACTB) in Human Cancers," *Bioengineered* 12 (2021): 6166–6185.

29. W. Qi, J. Li, X. Pei, Y. Ke, Q. Bu, and X. Ni, "β-Actin Facilitates Etoposide-Induced p53 Nuclear Import," *Journal of Biosciences* 45 (2020): 34.

30. H. K. Wang, Y. T. Su, Y. C. Ho, et al., "HDAC1 Is Involved in Neuroinflammation and Blood–Brain Barrier Damage in Stroke Pathogenesis," *Journal of Inflammation Research* 16 (2023): 4103–4116.

31. W. Wang, X. Chen, J. Chen, et al., "Engineering Lentivirus Envelope VSV-G for Liver Targeted Delivery of IDOL-shRNA to Ameliorate Hypercholesterolemia and Atherosclerosis," *Molecular Therapy—Nucleic Acids* 35 (2024): 102115.

32. S. Rehman, S. Bishnoi, R. Roy, et al., "Emerging Biomedical Applications of the Vesicular Stomatitis Virus Glycoprotein," *ACS Omega* 7 (2022): 32840–32848.

33. W. Li, T. Ali, C. Zheng, et al., "Fluoxetine Regulates eEF2 Activity (Phosphorylation) via HDAC1 Inhibitory Mechanism in an LPS-Induced Mouse Model of Depression," *Journal of Neuroinflammation* 18 (2021): 38.

34. Y. Fan, C. Pionneau, F. Cocozza, et al., "Differential Proteomics Argues Against a General Role for CD9, CD81 or CD63 in the Sorting of Proteins Into Extracellular Vesicles," *Journal of Extracellular Vesicles* 12 (2023): e12352.

35. L. Yin, Y. Ye, L. Zou, et al., "AR Antagonists Develop Drug Resistance Through TOMM20 Autophagic Degradation-Promoted Transformation to Neuroendocrine Prostate Cancer," *Journal of Experimental & Clinical Cancer Research* 42 (2023): 204.

36. A. S. Monzel, J. A. Enríquez, and M. Picard, "Multifaceted Mitochondria: Moving Mitochondrial Science Beyond Function and Dysfunction," *Nature Metabolism* 5 (2023): 546–562.

37. T. Liu, Z. Juan, B. Xia, et al., "HSP70 Protects H9C2 Cells From Hypoxia and Reoxygenation Injury Through STIM1/IP3R," *Cell Stress & Chaperones* 27 (2022): 535–544.

38. Y. Liu, Y. Zhao, R. Tang, X. Jiang, Y. Wang, and T. Gu, "Effect of TFAM on ATP Content in Tachypacing Primary Cultured Cardiomyocytes and Atrial Fibrillation Patients," *Molecular Medicine Reports* 22 (2020): 5105–5112.

39. Z. Zhang, M. Zhou, H. Liu, W. Liu, and J. Chen, "Protective Effects of Shen Yuan Dan on Myocardial Ischemia-Reperfusion Injury via the Regulation of Mitochondrial Quality Control," *Cardiovascular Diagnosis and Therapy* 13 (2023): 395–407.

40. X. Lin, Y. Zhou, and L. Xue, "Mitochondrial Complex I Subunit MT-ND1 Mutations Affect Disease Progression," *Heliyon* 10 (2024): e28808.

41. D. Milenkovic, J. Misic, J. F. Hevler, et al., "Preserved Respiratory Chain Capacity and Physiology in Mice With Profoundly Reduced Levels of Mitochondrial Respirasomes," *Cell Metabolism* 35 (2023): 1799–1813.e7.

42. H. Bugger and K. Pfeil, "Mitochondrial ROS in Myocardial Ischemia Reperfusion and Remodeling," *Biochimica et Biophysica Acta, Molecular Basis of Disease* 1866 (2020): 165768.

43. C. Li, H. Song, C. Chen, et al., "LncRNA PVT1 Knockdown Ameliorates Myocardial Ischemia Reperfusion Damage via Suppressing Gasdermin D-Mediated Pyroptosis in Cardiomyocytes," *Frontiers in Cardiovascular Medicine* 8 (2021): 747802.

44. Y. Cen, W. Liao, T. Wang, and D. Zhang, "APPL1 Ameliorates Myocardial Ischemia–Reperfusion Injury by Regulating the AMPK Signaling Pathway," *Experimental and Therapeutic Medicine* 23 (2022): 157.

45. J. Zheng, Z. Mao, J. Zhang, L. Jiang, and N. Wang, "Paeonol Pretreatment Attenuates Anoxia-Reoxygenation Induced Injury in Cardiac Myocytes via a BRCA1 Dependent Pathway," *Chemical & Pharmaceutical Bulletin* 68 (2020): 1163–1169.